Journal of Applied Electrochemistry **32**: 629–634, 2002.

Effects of boric acid on hydrogen evolution and internal stress in films deposited from a nickel sulfamate bath

Y. TSURU[1], M. NOMURA[1] and F.R. FOULKES[2]*
[1]*Department of Materials Science and Engineering, Kyushu Institute of Technology, 1-1, Sensui, Tobata, Kitakyushu, 804, Japan*
[2]*Department of Chemical Engineering and Applied Chemistry, University of Toronto, Toronto, Ontario, M5S 3E5, Canada*
*(*author for correspondence)*

Received 22 October 1998; accepted in revised form 16 April 2002

Key words: boric acid, hydrogen evolution, internal stress, nickel films, nickel sulfamate bath

Abstract

The effects of boric acid additions on the pH close to the electrode surface, on the hydrogen evolution reaction and on the internal stress in the plated films were studied for the high speed electroplating of nickel from a nickel sulfamate bath at a current density close to the nickel ion limiting current density. The study was carried out at 50 °C and pH 4.0 using a 1.55 M nickel sulfamate plating bath containing boric acid at concentrations ranging from 0 to 0.81 mol L^{-1}. The variation of the internal strain in the plated nickel films was determined *in situ* using a resistance wire-type strain gauge fitted to the reverse side of the copper electrode substrate. The solution pH at a distance of 0.1 mm from the depositing nickel film was measured *in situ* using a miniature pH sensor assembly consisting of a thin wire-type antimony electrode and a Ag/AgCl/sat. KCl electrode housed in a thin Luggin capillary. The addition of boric acid was shown to effectively suppress the hydrogen evolution reaction at nickel electrodeposition rates (18.0 A dm^{-2}) close to the limiting current density (~20 A dm^{-2}). Consequently, the solution pH adjacent to the plating metal surface was maintained at a value close to that in the bulk solution and the development of high internal stresses in the deposited nickel films was avoided.

1. Introduction

The industrial mass-production of electronic devices has created a demand for high speed electroplating. In particular, high speed nickel electroplating is currently being used as a micro-electroforming technique for the production of electronic contact elements such as bumps in integrated circuits and for the production of components for micromachines [1, 2]. Nickel sulfamate baths containing boric acid are widely used for the high speed electroplating of nickel because it is easier to obtain thick deposits with less internal tensile stress from these baths than from Watts-type baths.

The function of boric acid during nickel electroplating has been studied by previous researchers by applying potentiometric titration procedures to the plating baths or by studying the effects of solution pH on the potential–current curves for nickel electroplating. Their results may be summarized into the following five views: (a) *Boric acid acts as a pH buffering reagent* [3, 4]. The practical pH range of a buffer is $pK_a \pm 1$, which, in the case of boric acid (at 25 °C) is 9.23 ± 1. This clearly is too high a value in view of the fact that the bulk pH of the nickel plating bath is 4.0. Saubestre [5] and Tilak [6] explained this inconsistency by suggesting that some weakly bound complex might form between boric acid and nickel ions, and that it is this complex that acts as the pH buffering reagent. However, the existence of such a complex has not been confirmed experimentally. (b) *Boric acid acts as a catalyst for nickel deposition*. Hoare [7], based on the results of cyclic voltammetric experiments, reported that as the boric acid concentration increased, the rate of nickel deposition increased relative to the rate of hydrogen evolution. However, our own studies of steady state nickel electrodeposition have shown that the partial nickel deposition current density *vs.* potential curves are relatively unaffected by the levels of boric acid addition [8]. (c) *Boric acid suppresses hydrogen evolution*. Horkans [9] has claimed that boric acid adsorbs on the nickel surface during plating and significantly suppresses hydrogen evolution. (d) *Boric acid accelerates the deposit growth rates*. Abyaneh [10] has reported that the use of boric acid as a buffer increases both the outward and the lateral growth rate of nickel deposition. (e) *Boric acid reduces passive film formation in nickel electroplating*. Yin [11] has claimed that boric acid prevents the electrode surface from passivating during nickel reduction and acts as a surface agent.

From our own studies of nickel electroplating from Watts-type baths we have shown the following [8, 12]. (i) Boric acid acts as a pH buffering reagent mainly at current densities less than 1.0 A dm^{-2}. (ii) At nickel electroplating current densities greater than 3.0 A dm^{-2}, boric acid effectively suppresses hydrogen evolution and helps to suppress the development of high internal stresses in the plated nickel films. (iii) This ability of boric acid to suppress hydrogen evolution is observed only in the presence of nickel ion, indicating the involvement of some kind of mutual interaction between boric acid and a nickel-containing intermediate formed during the deposition process. (iv) The formation of a passive film on the nickel surface tends to result in an increase in the internal stress in nickel films deposited during periodic reversed current electrolysis.

To clarify the role of boric acid, in the present study we report on the effects of boric acid additions on hydrogen evolution and on the internal stresses in nickel films plated during high speed electroplating from a sulfamate bath operated near the nickel ion limiting current density.

2. Experimental details

Table 1 shows the composition of the sulfamate baths employed. Electroplating was carried out at 50 °C using a galvanostatic method without stirring in a beaker-type cell containing 150 mL of solution. For each experiment, 120 C of electricity (corresponding to a film thickness of approximately 20 μm) was passed through the cell. Fresh electrolyte was used for each experiment. The substrate metal for the electroplating consisted of 0.6 mm thick commercial copper sheet (99.9% Cu), which was cut into the appropriate size and annealed at 350 °C for 2 h in a vacuum. The electrode was masked to expose an electrode area 25 mm long by 8 mm wide. After electropolishing at room temperature in 50 vol % phosphoric acid for about 5 min, the electrode was immersed vertically into the bath with its exposed surface facing the surface of the counter electrode, the latter consisting of a commercial nickel plate of 99.99% purity. All the potentials are measured and reported with respect to the Ag/AgCl/sat. KCl reference electrode (0.197 V *vs* SHE at 25 °C).

The average internal strain in a given deposit was determined *in situ* using a resistance wire-type strain gauge fitted to the reverse side of the copper substrate. The expansion and contraction of the strain gauge with the bending of the copper substrate during electroplating can be assumed to precisely reflect the residual stress in the deposited nickel film [13, 14].

The solution pH at a distance of 0.1 mm from the surface of the deposited film was measured *in situ* using a specially constructed miniature pH sensor comprising a small antimony electrode combined with a small Ag/AgCl/sat. KCl electrode [15, 16]. The antimony electrode consisted of a 5 μm thick layer of antimony deposited onto the tip of a PTFE-insulated 0.1 mm diameter stainless steel wire in such a way that only the antimony was exposed to the solution. The accompanying Ag/AgCl/sat. KCl electrode was housed in a 0.1 mm diameter glass Luggin capillary, which was fixed at a distance of 0.5 mm below the antimony electrode. The pH sensor was connected to a micrometer-head which permitted the antimony tip to be moved horizontally with a precision of 10 μm to 0.1 mm from the surface of the nickel film during plating.

The IR-drop was measured using a Hokuto Denko model HC-110 current interrupter, with a distance of 2 mm being maintained between the Luggin capillary and the surface of the nickel cathode. The amount of nickel deposited was determined by dissolving the nickel film in acid and analysing the resulting solution using atomic absorption. The crystal structure of the deposit was evaluated using X-ray diffraction (XRD), while its morphology was examined using scanning electron microscopy (SEM).

Table 1. Composition of nickel sulfamate baths used for high speed electroplating

Bath	A	B	C	D	E
$Ni(OSO_2NH_2)_2$	1.55 M	1.55 M	1.55 M	1.55 M	1.55 M
H_3BO_3	0	0.08 M	0.16 M	0.49 M	0.81 M
pH	4.0	4.0	4.0	4.0	4.0

M = mol dm^{-3}.

3. Results and discussion

3.1. *Potential–partial current density curves for nickel electroplating*

The limiting current density for the metal ions can be evaluated from the IR-free potential–partial current density curve for the metal deposition process. Figure 1

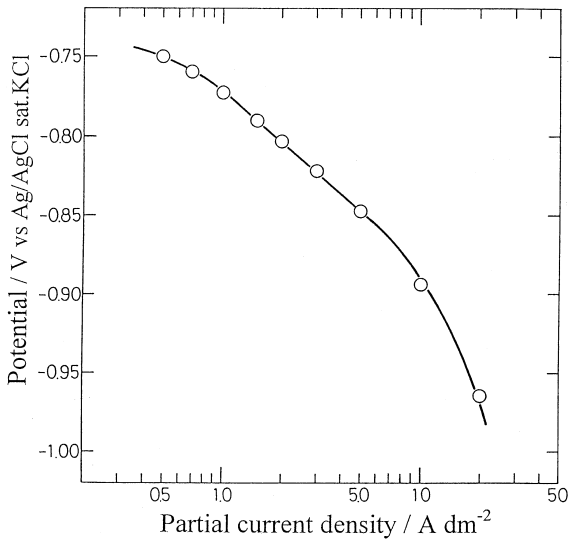

Fig. 1. IR-free potential–partial current density curve for nickel deposition from bath E.

shows this curve for nickel electroplating from bath E, containing 0.81 M H_3BO_3. The curve indicates that the process typically exhibits a tafel slope of −0.12 V (decade)$^{-1}$, and that the limiting current density for the nickel ions in bath E is around 20–25 A dm^{-2}.

The observed tafel slope of −0.12 V (decade)$^{-1}$ is the same value as that reported by Epelboin [17] for a Watts-type bath. Using a chemical impedance technique, Epelboin found evidence for the following reaction mechanism in which the rate-determining step (RDS) involves an intermediate species postulated to be $(NiOH)_{ads}$ [18]:

$$Ni^{2+} + H_2O \leftrightharpoons NiOH^+ + H^+$$

$$NiOH^+ + e^- \xrightarrow{RDS} (NiOH)_{ads}$$

$$(NiOH)_{ads} + H^+ + e^- \leftrightharpoons Ni + H_2O$$

The fact that the same tafel slope also is observed in the present work suggests that a similar $(NiOH)_{ads}$ species might be formed as an intermediate which adsorbs on the electrode surface during the electroplating of nickel from a sulfamate bath as well as from a Watts-type bath.

3.2. *Effects of current density on internal strain and stress*

Figure 2 shows the relationship between the cathodic current density and the average internal strain in nickel films plated from bath E, containing 0.81 M H_3BO_3. The internal strain increased with increasing current density and with the integrated quantity of electricity passed during electrodeposition.

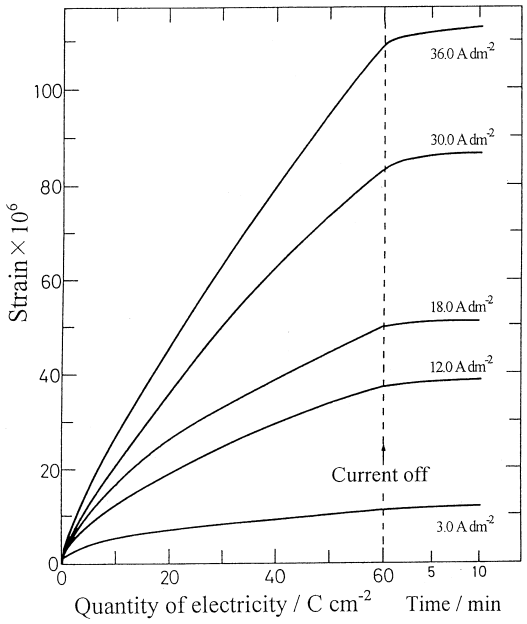

Fig. 2. Relation between cathodic current density and average internal strain in nickel films plated from bath E.

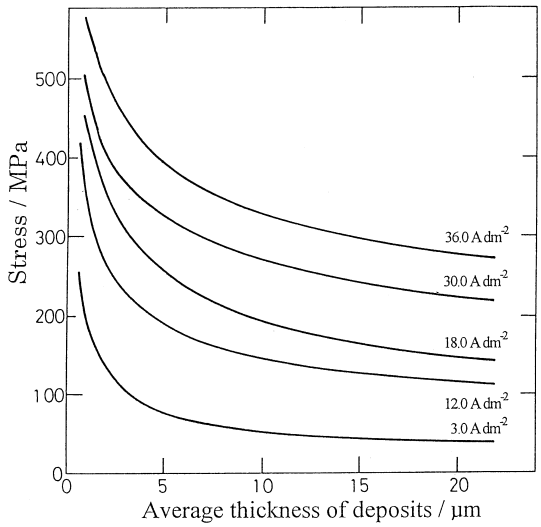

Fig. 3. Relation between average thickness and internal stress for nickel films plated from bath E.

The internal stress in a plated metal film can be calculated from the internal strain when the values of Young's modulus and Poisson's ratio for the metal are known [19]. Figure 3 shows the results of such calculations for the internal stress as a function of average nickel film thickness and plating current density. The data in Figure 3 were calculated from the strain data of Figure 2 using values for Young's modulus of 201.0 GPa and 122.6 GPa for the nickel film and the copper substrate, respectively; similarly, the corresponding respective values of Poisson's ratio were taken as 0.31 and 0.34 [20, 21]. It is seen from Figure 3 that at a plating current density of 3.0 A dm^{-2} the internal tensile stress in a 20 μm thick nickel film was only about 40 MPa, rising only to about 275 MPa even at the high current density of 36.0 A dm^{-2}.

The XRD patterns of the plated nickel films are shown in Figure 4. All the films consisted of nickel

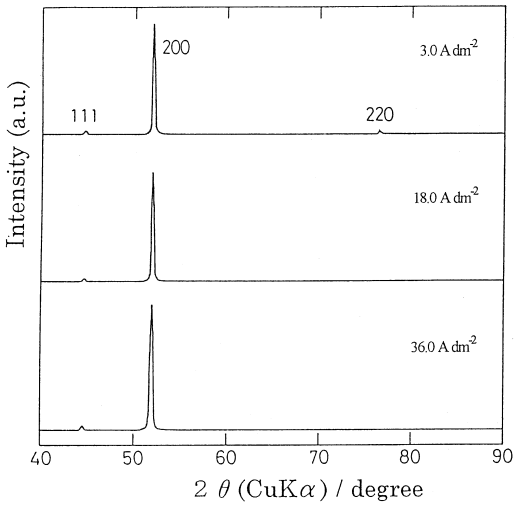

Fig. 4. X-ray diffraction patterns of nickel films plated from bath E at various current densities.

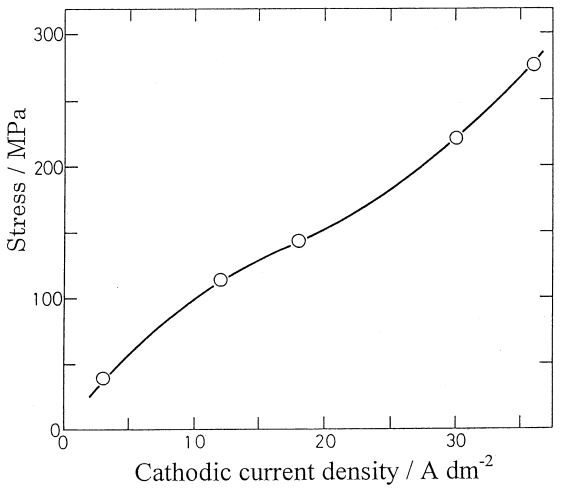

Fig. 5. Effect of current density on stress for 20 μm thick nickel films plated from bath E.

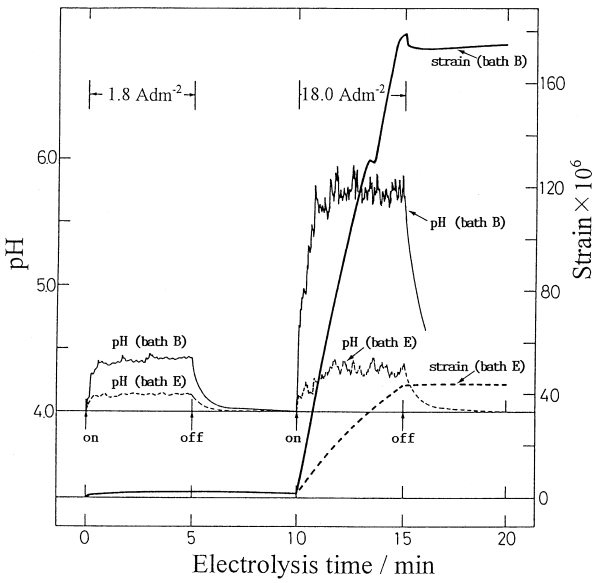

Fig. 6. Relation between pH of solution at 0.1 mm from electrode surface and internal strain in nickel films plated from bath B (0.08 M H_3BO_3) and bath E (0.81 M H_3BO_3).

crystals with a {2 0 0} preferred orientation. In general, plated nickel films with relatively low tensile stress tend to exhibit a {2 0 0} preferred orientation [8].

Figure 5 shows that the internal stress gradually increased linearly with an increase in the current density up to a current density of about 20 A dm^{-2}, which approximately corresponds to the nickel ion limiting current density. Throughout this current density region the current efficiency was almost constant at close to 100% (cf. Table 2). However, at current densities greater than about 20 A dm^{-2}, the internal tensile stress started to increase with current density at an increasingly steeper rate, while the current efficiency slowly started to decrease. Brown [22] reported that the current efficiency for nickel electroplating from a Watts-type bath also was almost 100% at high current densities approaching the limiting current density. He speculated that, in addition to its pH buffering action, boric acid must play some important role during nickel electroplating. Thus, the accelerated increase in the internal stress (Figure 5) at current densities greater than 20–25 A dm^{-2} and the accompanying decrease of the current efficiency from 100% (Table 2) would appear to be related to the influence of the nickel ion limiting current density. Consequently, the observed sudden increase in the internal stress can be attributed to the onset of hydrogen evolution during the nickel deposition process.

3.3. *Solution pH close to the electrode and internal strain*

Figure 6 shows the relationship between the solution pH (dynamically measured during the actual plating process) at a distance of 0.1 mm from the surface of the nickel cathode and the internal strain developed in the resulting nickel films deposited from bath B (0.08 M H_3BO_3) and from bath E (0.81 M H_3BO_3). The measurements of both solution pH and internal strain were carried out at a plating current density of 18.0 A dm^{-2}, following the initial deposition at 1.8 A dm^{-2} of a preliminary nickel film of 1.8 μm thickness. During electrodeposition from bath E, containing a high concentration of boric acid (0.81 M), the pH next to the electrode surface remained close to the bulk solution value of 4.0; however, for bath B, containing only 0.08 M H_3BO_3, the pH adjacent to the electrode surface rose rapidly to a value of about 5.75, concurrent with the precipitation of nickel hydroxide [23]. Raub [24] has reported that the precipitation of nickel hydroxide in a Watts-type bath begins at a solution pH of 5.0 to 5.6, which then fluctuates around this value in step with the release of hydrogen bubbles from the electrode surface.

The resulting strain generated in the nickel film deposited from the low boric acid concentration bath was four times as high as that developed in the high boric acid concentration bath. The hydroxyl ion generated during the hydrogen evolution process via

$$H_2O + e^- \rightarrow \tfrac{1}{2}H_2 + OH^-$$

accounts for the general observation that the higher the solution pH, the greater will be the internal strain found in the plated metal film [25, 26]. In the case of bath B, although the pH in the bulk of the bath was maintained at the low value of 4.0, the high pH value of about 6 adjacent to the electrode surface indicates the presence of significant hydrogen generation at the metal surface, and, consequently, explains the significant increase in the observed internal strain in the resulting nickel film.

Table 2. Effect of plating current density on current efficiency for 20 μm thick nickel films deposited from bath E

Current density/A dm^{-2}	3.0	6.0	18.0	36.0	45.0	60.0
Current efficiency/%	98.8	99.8	99.9	99.4	98.8	96.2

On the other hand, as we have shown above, a high concentration of boric acid in the plating bath is able to suppress hydrogen evolution during nickel electroplating. Therefore, as indicated by the failure of the pH next to the electrode surface to increase significantly beyond the bulk value of pH 4.0, the high concentration of boric acid in bath E was able to effectively suppress the generation of hydrogen at the electrode surface, resulting in the suppression of increased internal strain, and hence stress, in the nickel film.

3.4. *Effect of boric acid on internal strain and stress*

Figure 7 shows the effect of the concentration of boric acid in the bath on the internal strain in nickel films plated at a current density of 18.0 A dm^{-2}. At boric acid concentrations $\geqslant 0.16$ M (baths C, D, and E) the internal strain smoothly increased with the total quantity of electricity passed during a given run. However, in the case of bath A, which contained no boric acid, the internal strain increased in a fluctuating, unpredictable manner relative to that observed with the baths containing boric acid. Figure 8 shows the relationship between the average thickness of the plated nickel film and the internal stress calculated from the strain curves of Figure 7, using the same values as those used earlier for Young's modulus and Poisson's ratio for nickel and copper. It is clear from Figure 8 that as the boric acid concentration is lowered from the typical industrial value of 0.81 M (Bath E, 50 g L^{-1}), there is a significant increase in internal stress in the nickel film. An interesting feature of bath A, containing no boric acid, is the discernible shoulder which always appears in the stress–thickness curve.

Figure 9 shows the surface morphology of the plated nickel films. The film plated from bath C (0.16 M H_3BO_3) consisted of a typical block-and-pyramid-like

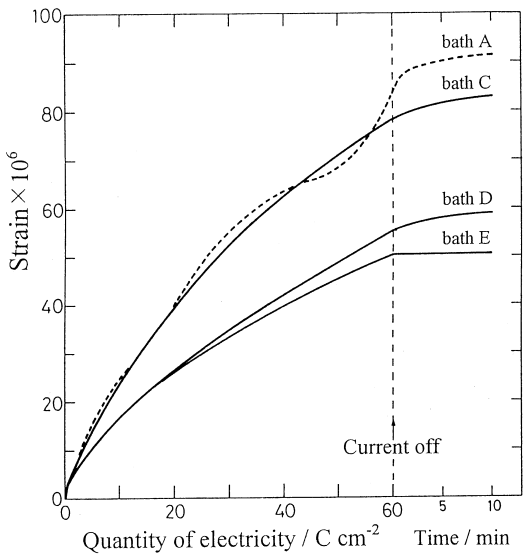

Fig. 7. Effects of boric acid concentration on internal strain in nickel films plated at 18.0 A dm^{-2}.

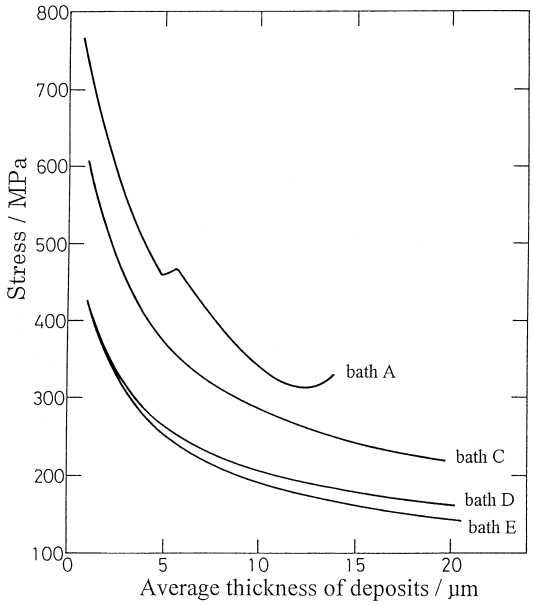

Fig. 8. Relationship between average thickness of nickel film and internal stress.

nickel deposit. However, in the absence of boric acid (bath A) the morphology of the plated nickel film changed to a compact deposit with many cracks. Because such cracks tend to appear when the internal tensile stress in the plated nickel film overcomes its yield strength, the shoulders discernible in the stress–thickness curves obtained using bath A would appear to be a manifestation of crack initiation and growth. Figure 10 shows the effect of boric acid concentration on the current efficiency at a cathodic current density of 18.0 A dm^{-2}. As the concentration of boric acid in the bath is decreased from 0.81 M (bath E) to about 0.16 M (bath C), the current efficiency slowly falls from close to 100% to about 97%. However, at concentrations lower than about 0.08 M (bath B), the current efficiency rapidly falls with decreasing boric acid concentration, dropping to a value of only 63% when no boric acid is present (bath A). The increase in internal stress shown in Figure 8 correlates with this decrease in current efficiency, indicating that, at current densities close to the limiting current density, the presence of boric acid in the bath somehow inhibits hydrogen evolution, and, consequently, suppresses an increase in the internal tensile stress generated in the plated nickel film.

Armyanov [27, 28] has claimed that the desorption of hydrogen codeposited in the nickel electroplated from a Watts-type bath containing 2-butyne-1,4-diol as additive is responsible to a considerable extent for the tensile stress in the films. The spontaneous increase of strain in the nickel films after the current is switched off in Figures 2 and 7 might be consistent with the phenomenon observed in his investigations of the correlation between internal stress and hydrogen. However, the existence of nickel hydride deposits has been confirmed *in situ* using X-ray diffraction in a low temperature electroplating study [24]; also, the phase transformation

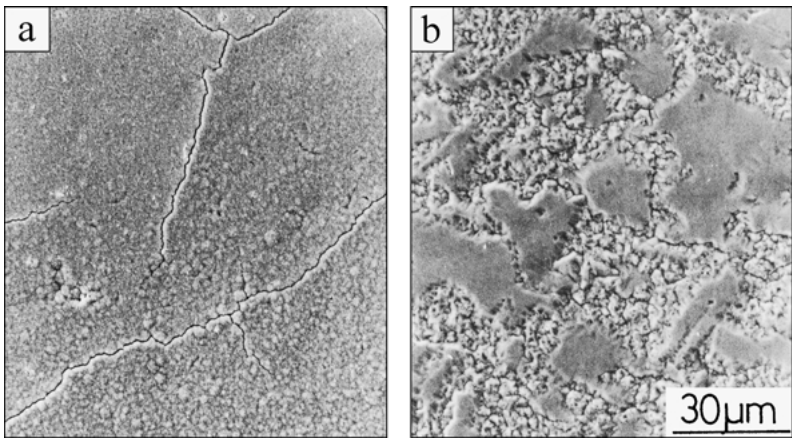

Fig. 9. Effects of boric acid concentration on surface morphology of nickel films plated at 18.0 A dm^{-2}: (a) bath A (no boric acid) (b) bath C (0.16 M H_3BO_3).

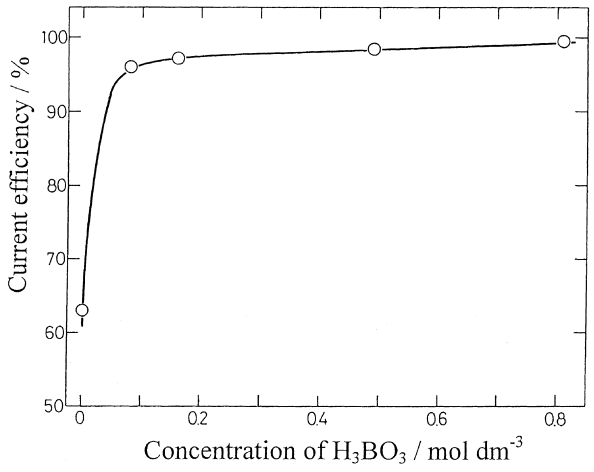

Fig. 10. Effect of boric acid concentration on current efficiency for nickel electroplating at 18.0 A dm^{-2}.

of nickel into unstable nickel hydride has been observed during cathodic charging of electroplated bright nickel films in an acidic medium [29, 30].

4. Conclusions

Boric acid effectively suppresses hydrogen evolution during high speed nickel electroplating from a sulfamate bath near the limiting nickel ion diffusion current density. Consequently, the pH adjacent to the plating metal surface is maintained at a value close to that in the bulk solution, so that the deleterious effects of hydrogen codeposited during electroplating on the development of high internal stresses in the resulting nickel films are greatly reduced.

References

1. W. Ehrfeld, *in* H. Reicl (Ed.), Proceedings of 1st International Conference on 'Micro Electro, Opto, Mechanic Systems and Components', Micro System Technologies 90 (Springer-Verlag, Berlin, Sept. 1990), pp. 521–528.
2. H. Honma, H. Watanabe and T. Fujinami, *in* Proceedings of 14th World Congress on 'Interfinish', Interfinish 96 (Birmingham, UK, Sept. 1996), Vol. 3, pp. 347–358.
3. A.H. DuRose, *Plat. Surf. Finish.* **64** (Aug. 1977) 52.
4. J. Ji, W.C. Cooper, D.B. Dreisinger and E. Peters, *J. Appl. Electrochem.* **25** (1995) 642.
5. E.B. Saubestre, *Plating* **45** (1958) 927.
6. B.V. Tilak, A.S. Gendron and M.A. Mosoiu, *J. Appl. Electrochem.* **7** (1977) 495.
7. J.P. Hoare, *J. Electrochem. Soc.* **133** (1986) 2491; **134** (1987) 3102.
8. Y. Tsuru, R. Takamatsu and K. Hosokawa, *J. Surf. Finish. Japan* **44** (1993) 39; **45** (1994) 82.
9. J. Horkans, *J. Electrochem. Soc.* **126** (1979) 1861.
10. M.Y. Abyaneh and M. Hashemi-Pour, *Trans. IMF* **72** (1993) 23.
11. K-M. Yin and B-T. Lin, *Surf. Coat. Technol.* **78** (1996) 205.
12. Y. Tsuru, T. Tamai and K. Hosokawa, *in* Proceedings of 14th World Congress on 'Interfinish', Interfinish 96 (Birmingham, UK, Sept. 1996), Vol. 2, pp. 89–99.
13. G. Fischer, *Galvanotechnick* **53** (1962) 335.
14. Y. Tsuru, M. Nomura and F.R. Foulkes, *J. Appl. Electrochem.* **30** (2000) 231.
15. Y. Tsuru, K. Yamabe and K. Hosokawa, *J. Surf. Finish. Japan* **40** (1989) 345.
16. T. Honda, K. Murase, T. Hirato and Y. Awakura, *J. Appl. Electrochem.* **28** (1998) 617.
17. I. Epelboin and R. Wiart, *J. Electrochem. Soc.* **118** (1971) 1577.
18. J. Matulis and R. Slizys, *Electrochim. Acta* **9** (1964) 1177.
19. Y. Shibasaki, *Denki Kagaku*, **19** (1951) 320.
20. W.H. Safranek, 'The Properties of Electrodeposited Metals and Alloys', 2nd edn (American Electroplaters and Surface Finishing Society, USA, 1986), pp. 291–293.
21. H.M. Ledbetter, *Mater. Sci. Eng.* **27** (1977) 133.
22. H. Brown and B.B. Knapp, 'Modern Electroplating', 3rd edn (J. Wiley & Sons, New York, 1974), p. 289.
23. Y. Tsuru and S. Oono, *J. Surf. Finish. Japan* **50** (1999) 202.
24. Ch. J. Raub, *Plat. Surf. Finish.* **80** (September 1993) 30.
25. S. Konishi, *Metal Finish.* **63** (April 1965) 67.
26. R. Weil, *Plating*, **58** (1971) 50.
27. S. Armyanov and G. Sotirova-Chakarova, *Surf. Coat. Technol.* **34** (1988) 441.
28. S. Armyanov and G. Sotirova-Chakarova, *J. Electrochem. Soc.* **139** (1992) 3454.
29. R. Juskenas, A. Selskis and V. Kadziauskiene, *Electrochim. Acta* **43** (1998) 1903.
30. M. Monev, *Electrochim. Acta* **46** (2001) 2373.